Successive ionic layer deposition of Co-doped Cu(OH)$_2$ nanorods as electrode material for electrocatalytic reforming of ethanol

I. A. Kodintsev[1*], K. D. Martinson[1], A. A. Lobinsky[2], V. I. Popkov[1]

[1]Ioffe Institute, 194021 Saint Petersburg, Russia
[2]Saint Petersburg State University, Peterhof, 198504 Saint Petersburg, Russia

*i.a.kod@mail.ru

In this work, a facile and cost-effective layer by layer method was proposed to synthesize novel high stable and effective electrode material based on the Co-doped Cu(OH)$_2$ nanocrystals. The crystals have orthorhombic structure and a rod-like morphology with a 23 ± 2 nm in width and 43 ± 4 nm in length. The composition of the nanocrystals corresponds to the 1 % Co-doped Cu(OH)$_2$ by EDX with no noticeable impurities as it was found by FTIR spectroscopy. It was shown that nickel electrode modified with nanorods is characterized by an overvoltage value of -347 mV at 10 mA/cm^2, which is 250 mV lower than that of an initial pure nickel electrode. The value of Tafel slope that reaches 138 mV/dec, high stability of the Co-doped Cu(OH)$_2$ nanorods in chronopotentiometric (10 hours) and cyclic volamperometric (500 cycles) tests allows us to consider them as a prospective basis of electrode materials for the hydrogen evolution from renewable water-alcohol sources.

1. Introduction

The interest in the development of a clean and renewable energy source has been increased over the last few decades due to increased energy needs, the depletion of fossil fuel reserves and environmental pollution. Hydrogen is most often considered as such energy source [1]. There are various methods of hydrogen production, such as steam reforming [2], water electrolysis [3,4], biological processes [5] and photoelectrolysis [6,7]. In recent years, a method of hydrogen production from water-alcohol mixtures (or, as it is called electrochemical reforming or ECR) is being developed as an alternative technique to the water electrolysis because of the lower energy requirements [8]. However, the wide application of this method is limited because of the scarcity and high cost of Pt electrodes. Thus, the alternative electrode materials are the main research objective in this area.

Various cost-efficient nanomaterials have been developed for hydrogen evolution reactions, including oxides [9, 10] sulfides [11–13], phosphides [14–16], carbides [17], nitrides of d-elements [18], and composites with other materials [19–21]. However, among them, Cu-based materials are much less explored for hydrogen evolution, due to the instability and low catalytic efficiency, despite the fact that such materials have much higher electrical conductivity [22]. Those Cu-based materials seem to be promising electrode materials, basic for the ECR process, in the cases of solving the problem of their effective production and increasing of their functional characteristics.

There are two main strategies for improving the hydrogen evolution performance of Cu-based materials: the first one is to form nanocomposites by heteroatom doping; and the second is to construct nanostructures with specific morphologies with high surface area, such as nanowires, nanotubes, and nanosheets [23–25]. Both of strategies, as it will be shown below, can be attained by using successive ionic layer deposition (SILD) which is a kind of layer-by-layer methods [26,27].

The layer-by-layer method is one technique that allows the synthesis of the nanocomposites mentioned above [28–30]. It is based on the sequential absorption of precursors on the substrate surface, followed by the removal of excess reagents. The result is a film of the synthesized substance, the thickness of which increases with repetition of adsorption reactions in proportion to the number of processing cycles [31]. This approach allows one to synthesize nanoparticles with non-isometric morphology and to finely vary their composition by changing the composition of the reaction solutions. So, the aim of this work is to investigate the structure and electrochemical properties of Co-doped Cu(OH)$_2$ non-isometric nanoparticles, synthesized via the SILD method, and the possible use of this nanocomposite as a suitable material for hydrogen evolution via electrochemical reforming of the water-ethanol solution.

2. Experimental

Monocrystalline silicon plates with the orientation of [100] and nickel foam plates (JSC ECAT, 90 PPI) with the size of 5×20 mm were used as substrates for nanocomposite synthesis. Before synthesis, these plates were treated in acetone for 10 minutes in an ultrasonic bath. Then, silicon plates were etched with concentrated HF for 15 minutes and nickel foam plates were treated with 6 M HCl solution for 15 minutes. After that, the silicon plates were treated for 20 minutes in dilute aq. KOH solution with pH = 9.0. Finally, all wafers were washed with deionized water and air-dried at $80°$ for 30 minutes.

The nanocomposite was synthesized on the substrates using a layer-by-layer technique. During the synthesis, the wafers were immersed for 30 seconds into the solution containing 0.1 M $Cu(CH_3COO)_2$ and 0.01 M $Co(CH_3COO)_2$, distilled water, solution of NaOH with pH = 9 and again distilled water. This treatment considered as one layer-by-layer cycle.

The elemental analysis and morphology of the synthesized sample were studied by energy dispersive X-ray analysis (EDX) and scanning electron microscopy (SEM) using Tescan Vega 3 SBH scanning electron microscope equipped with an Oxford INCA x-act X-ray microanalysis device. X-ray phase analysis was performed on a RigakuSmartLab 3 X-ray powder diffractometer, phase analysis of the composition was performed using ICDD PDF-2 powder database. The average crystallite size (coherent-scattering regions) was calculated from the broadening of X-ray diffraction lines using the Scherrer formula. FTIR spectra were obtained using Shimadzu IRTracer-100 FTIR spectrometer in the spectral range from 350 cm^{-1} to 4000 cm^{-1} with a spectral resolution 2 cm^{-1}.

Electrochemical properties of obtained electrodes for electrochemical reforming were investigated using potentiostat Elins P-45X and a three-electrode cell. Nickel foam plate with nanocomposite film deposited via the layer-by-layer method was used as a working electrode, the Ag/AgCl electrode was used as reference electrode and a platinum foil was used as a counter electrode. All measurements have been carried out at atmospheric pressure and room temperature in aq. 1 M KOH solution with 10 % (by volume) ethanol as the electrolyte. The voltammogram was made at 5 mV/s sweep rate with IR compensation (1.3Ω). Chronopotentiogram was made at a current density of -10 mA/cm^2.

3. Results and discussions

According to the XRD pattern (Fig. 1), the only phase in the sample is copper (II) hydroxide $Cu(OH)_2$ with the orthorhombic structure (JCPDS 13-420) with *Cmcm* space group.
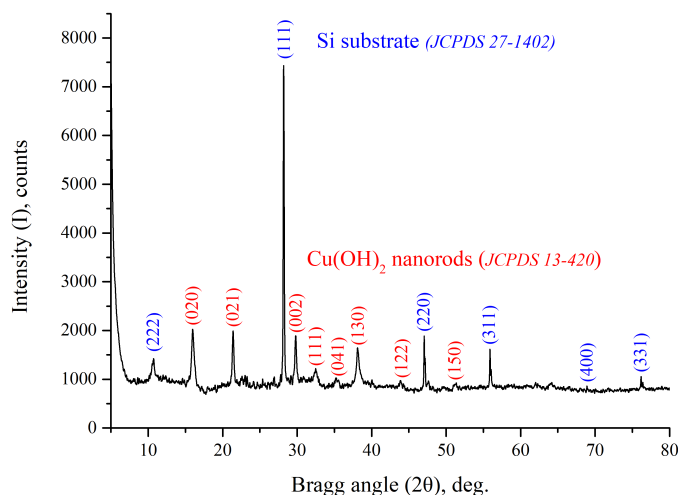
FIG. 1. XRD pattern of Co-doped $Cu(OH)_2$ nanorods on a silicon wafer

Refining of the unit cell parameters of this sample using Rietveld method yielded the following results: $a = 2.9489$ Å, $b = 11.1141$ Å, $c = 6.2414$ Å, $\alpha = \beta = \gamma = 90°$, $R_{wp} = 5.41$ %. A significant difference in the broadening of the X-ray diffraction lines in individual crystallographic directions indicates the anisotropic shape of the $Cu(OH)_2$ crystallites. Analysis of these data using the Scherrer formula allowed us to establish the size of coherent scattering region: in the [111] direction – 23 ± 2 nm, in the [002] direction – 43 ± 4 nm. Thus, taking into account

the exact arrangement of these crystallographic planes in crystals with an orthorhombic structure [32], it could be concluded that the obtained nanocrystals have a morphology of nanorods, which is also confirmed by scanning electron microscopy (Fig. 2(b,c,d)).
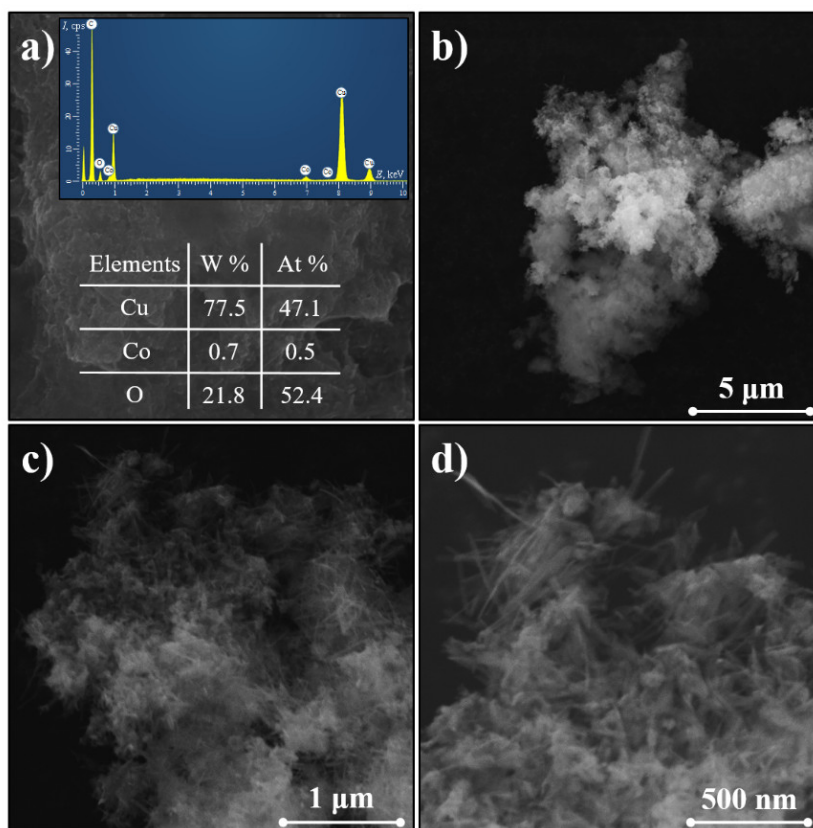
FIG. 2. a – EDX spectrum; b,c,d – SEM images of Co-doped Cu(OH)$_2$ nanorods on a silicon wafer

The results of scanning electron microscopy indicate that the synthesized nanocrystals of Co-doped Cu(OH)$_2$ are in the sample in the form of agglomerates with micron sizes (Fig. 2(a)). Only at a higher magnification, it becomes noticeable that each agglomerate consists of a large number of copper hydroxide nanorods. However, the nanorods observed on SEM images have a submicron length, which differs from the crystallite lengths, about 40 nm, estimated on the base of X-ray diffractometry data. Thus, these submicron nanorods are non-oriented intergrown nanocrystals of Co-doped Cu(OH)$_2$. The similar structure of micron and submicron rods based on intergrown nanocrystals was observed earlier in work [33]. The EDX analysis shows that synthesized nanocrystals include cobalt atoms with Cu/Co ratio equal to 99.0 %: 1.0 %. Thus, 1 % Co-doped Cu(OH)$_2$ nanorods were synthesized as a result of the successive ionic layer deposition.

Figure 3 shows the FT-IR spectra of the obtained nanocomposite. The strong and broad absorption band at around 3300 cm^{-1} and a sharp peak at 3571 cm^{-1} is attributed to the stretching mode of –OH groups, which indicates the presence of hydroxyls in the free water and in the copper hydroxides, correspondently. The bands at 913, 1358, and 1561 cm^{-1} are attributed to the bending mode of H$_2$O and CO$_2$ coordinated to metal ions [34] that is the result of adsorption of these substances by the developed surface of the hydroxide obtained. Three intense bands at 683, 610, and 512 cm^{-1} are attributed to Cu–O vibrations and additionally confirm the presence of copper hydroxide. No absorption bands were detected, associated with the presence of cobalt and only a subtle shift in the absorption bands of the Cu–O bonds was observed with respect to pure copper hydroxide [26].

The electrochemical investigations show that the synthesized nanocomposite could be successfully used in electrochemical reforming of ethanol. Electrocatalytic properties were characterized by cyclic voltammetry and chronopotentiometry shown in Fig. 4.

The overpotential of hydrogen evolution for the initial sample and the sample after 500 cycles of charge-discharge was determined from the polarization curves obtained at 5 mV/s scanning rate. The initial sample shows overpotential about -347 mV at current density 10 mA/cm^2. For the original nickel electrode, the overpotential value at this current
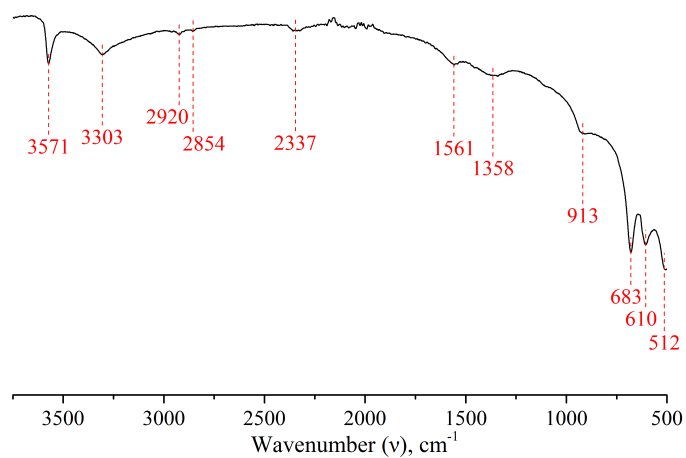
FIG. 3. FTIR spectrum of Co-doped Cu(OH)$_2$ nanorods
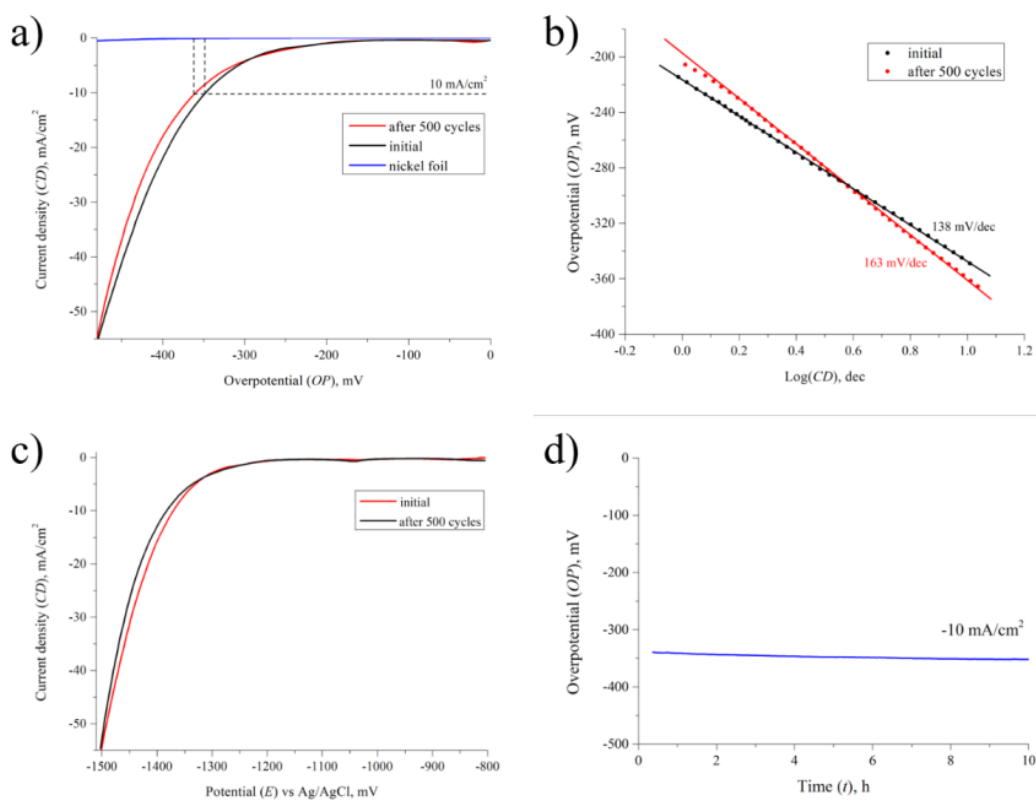
FIG. 4. a – polarization curves, b – Tafel slop, c – cyclic stability and d – chronoamperogramm of Co-doped Cu(OH)$_2$ nanorods

density is about -600 mV, thus the overvoltage on the cobalt-doped copper hydroxide electrode improved by 250 mV and approached the advanced electrode materials based on d-elements oxides [3, 4, 20]. A slight difference in the change of overpotential after 500 charge-discharge cycles indicates good electrochemical stability and low degradation of the obtained material.

The microkinetic characteristics of the samples were determined from the Tafel slope. The value of the Tafel slope was calculated using formula $\eta = a \cdot \log(i)$, where η – overpotential of HER reaction, i – current density, a – Tafel slope, from the linear part of the overpotential and it reaches 138 mV/dec and 163 mV/dec after 500 charge-discharge cycles (Fig. 4(b)). The obtained value of the Tafel slope is characteristic for electrocatalyst based on transition metal oxides and hydroxides during the HER reactions in an alkaline aqueous medium, as was previously noted [35]. It should be noted that after 500 charge-discharge cycles, the Tafel slope increases significantly (by 25 mV/dec), which indicates a change in the mechanism of hydrogen evolution from the catalyst surface. In our opinion, the observed effect may occur due to a change of surface morphology during cycling, at the same time the overvoltage changes insignificantly. The chronopotentiometry was used to characterize the stability of the material in a stationary mode at a given current density of 10 mA/cm^2. The measurements show that this nanocomposite is effective through all 10 hours of work and 500 cycles of voltammetry. Thus the results of electrocatalytic studies confirm that the Co-doped Cu(OH)$_2$ synthesized via successive ionic layer deposition can be considered as an effective and high stable material for hydrogen production by electrocatalytic reforming of water-ethanol solutions.

4. Conclusion

In this work, a successive ionic layer deposition method was used to synthesize Co-doped Cu(OH)$_2$ nanocrystals with rod-like morphology. As it was shown by XRD and SEM, nanocrystals of Co-doped Cu(OH)$_2$ have 23 ± 2 nm in width (for [111] crystallographic direction) and 43 ± 4 nm in length (for [002] crystallographic direction) and form agglomerates of the same width and micron-submicron length. The results of EDX, XRD and FTIR investigations confirmed the high purity of the synthesized Co-doped Cu(OH)$_2$ nanocrystals with Co content of 1 at. % in relation to Cu. Electrochemical investigation of the electrode with Co-doped Cu(OH)$_2$ shows overpotential values of 347 mV at a current density of 10 mA/cm^2 and Tafel slope values of 138 mV/dec for hydrogen evolution from water-ethanol solution (10 % v/v). In addition, it was found that the resulting electrode material has high stability in both chronoamperometry mode and in voltammetric cycling mode. On the base of this results, Co-doped Cu(OH)$_2$ nanorods synthesized via layer by layer approach, could be considered as a prospective basis of electrode materials for electrocatalytic reforming of ethanol.

References

[1] Ma T.Y., Dai S., Qiao S.Z. Self-supported electrocatalysts for advanced energy conversion processes. *Materials Today*, 2016, **19**, P. 265–273.

[2] Angeli S.D., Monteleone G., Giaconia A., Lemonidou A.A. State-of-the-art catalysts for CH$_4$ steam reforming at low temperature. *Int. J. Hydrogen Energy*, 2014, **39**, P. 1979–1997.

[3] Kelly N.A. *Hydrogen production by water electrolysis. Advances in Hydrogen Production, Storage and Distribution*. Woodhead Publishing, 2014, P. 159–185.

[4] Eftekhari A. Electrocatalysts for hydrogen evolution reaction. *Int. J. Hydrogen Energy*, 2017, **42**, P. 11053–11077.

[5] Das D., Veziroglu T.N. Hydrogen production by biological processes: a survey of literature. *Int. J. Hydrogen Energy*, 2001, **26**, P. 13–28.

[6] Huang Q., Li Q., Xiao X. Hydrogen evolution from Pt nanoparticles covered p-Type CdS: Cu photocathode in scavenger-free electrolyte. *J. Phys. Chem. C*, 2014, **118**, P. 2306–2311.

[7] Moha. Feroz Hossen, Abu Bakar Md. Ismail. Investigation on Fe$_2$O$_3$/por-Si photocatalyst for low-bias water-splitting. *J. Mater. Sci.: Mater. Electron.*, 2018, **29**, P. 15480–15485.

[8] Gutiérrez-Guerra N., Jiménez-Vázquez M., et al. Electrochemical reforming vs. catalytic reforming of ethanol: a process energy analysis for hydrogen production. *Chem. Eng. Process*, 2015, **95**, P. 9–16.

[9] Sun Z., Liao T., et al. Generalized self-assembly of scalable two-dimensional transition metal oxide nanosheets. *Nat. Commun.*, 2015, **5**, P. 3813.

[10] Lobinsky A.A., Tolstoy V.P. Synthesis of CoAl–LDH nanosheets and N-doped graphene nanocomposite via Successive Ionic Layer Deposition method and study of their electrocatalytic properties for hydrogen evolution in alkaline media. *J. Solid State Chem.*, 2019, **270**, P. 156–161.

[11] Huerta-Flores A.M., Torres-Martinez L.M., et al. Green synthesis of earth-abundant metal sulfides (FeS$_2$, CuS, and NiS$_2$) and their use as visible-light active photocatalysts for H$_2$ generation and dye removal. *J. Mater. Sci.: Mater. Electron.*, 2018, **29**, P. 11613–11626.

[12] Lukowski M.A., Daniel A.S., et al. Enhanced hydrogen evolution catalysis from chemically exfoliated metallic MoS$_2$ nanosheets. *J. Am. Chem. Soc.*, 2013, **135**, P. 10274–10277.

[13] Faber M.S., Dziedzic R., et al. High-performance electrocatalysis using metallic cobalt pyrite (CoS$_2$) micro- and nanostructures. *J. Am. Chem. Soc.*, 2014, **136**, P. 10053–10061.

[14] Yang X., Lu A.Y., et al. CoP nanosheet assembly grown on carbon cloth: a highly efficient electrocatalyst for hydrogen generation. *Nano Energy*, 2015, **15**, P. 634–641.

[15] Callejas J.F., McEnaney J.M., et al. Electrocatalytic and photocatalytic hydrogen production from acidic and neutral-pH aqueous solutions using iron phosphide nanoparticles. *ACS Nano*, 2014, **8**, P. 11101–11107.

[16] Liang Y., Liu Q., et al. Self-supported FeP nanorod arrays: a cost-effective 3D hydrogen evolution cathode with high catalytic activity. *ACS Catal.*, 2014, **4**, P. 4065–4069.

[17] Chen J., Zhou W., et al. Porous molybdenum carbide microspheres as efficient binder-free electrocatalysts for suspended hydrogen evolution reaction. *Int. J. Hydrogen Energy*, 2017, **42**, P. 6448–6454.

[18] Cao B., Veith G.M., et al. Mixed close-packed cobalt molybdenum nitrides as non-noble metal electrocatalysts for the hydrogen evolution reaction. *J. Am. Chem. Soc.*, 2013, **135**, P. 19186–19192.

[19] Kirillova S.A., Almjasheva O.V., Panchuk V.V., Semenov V.G. Solid-phase interaction in ZrO_2–Fe_2O_3 nanocrystalline system. *Nanosystems: Phys. Chem. Math.*, 2018, **9**, P. 763–769.

[20] Li J.S., Wang Y., et al. Coupled molybdenum carbide and reduced graphene oxide electrocatalysts for efficient hydrogen evolution. *Nat. Commun.*, 2016, **7**, 11204.

[21] Zvereva V.V., Popkov V.I. Synthesis of CeO_2–Fe_2O_3 nanocomposites via controllable oxidation of $CeFeO_3$ nanocrystals. *Ceramics International*, 2019, **45**, P. 1380–1384.

[22] Tran P.D., Nguyen M., et al. Copper molybdenum sulfide: a new efficient electrocatalyst for hydrogen production from water. *Energy Environ. Sci.*, 2012, **5**, P. 8912–8916.

[23] Yan Y., Xia B., Xu Z., Wang X. Recent development of molybdenum sulfides as advanced electrocatalysts for hydrogen evolution reaction. *ACS Catal.*, 2014, **4**, P. 1693–1705.

[24] Jaramillo T.F., Jorgensen K.P., et al. Identification of active edge sites for electrochemical H_2 evolution from MoS_2 nanocatalysts. *Science*, 2007, **317**, P. 100–102.

[25] Dasgupta A., Rajukumar L.P., et al. Covalent three-dimensional networks of graphene and carbon nanotubes: synthesis and environmental applications. *Nano Today*, 2017, **12**, P. 116–135.

[26] Kodintsev I., Reshanova K., Tolstoy V. Layer-by-layer synthesis of metal oxide (or hydroxide) – graphene nanocomposites. The synthesis of CuO nanorods – graphene nanocomposite. *AIP Conference Proceedings*, 2016, **1748**, 040005.

[27] Ehsan M.A., Naeem R., et al. Facile fabrication of CeO_2–TiO_2 thin films via solution-based CVD and their photoelectrochemical studies. *J. Mater. Sci.: Mater. Electron.*, 2018, **29**, P. 13209–13219.

[28] Popkov V.I., Tolstoy V.P., Omarov S.O., Nevedomskiy V.N. Enhancement of acidic-basic properties of silica by modification with CeO_2–Fe_2O_3 nanoparticles via successive ionic layer deposition. *Appl. Surf. Sci.*, 2019, **473**, P. 313–317.

[29] Bayram O., Simsek O., et al. Effect of the number of cycles on the optical and structural properties of Mn_3O_4 nanostructures obtained by SILAR technique. *J. Mater. Sci.: Mater. Electron.*, 2018, **29**, P. 10542–10549.

[30] Dmitriev D.S., Popkov V.I. Layer by layer synthesis of zinc-iron layered hydroxy sulfate for electrocatalytic hydrogen evolution from ethanol in alkali media. *Nanosystems: Phys. Chem. Math.*, 2019, **10**, P. 480–487.

[31] Lobinsky A.A., Tolstoy V.P., Kodinzev I.A. Electrocatalytic properties of gamma-NiOOH nanolayers, synthesized by successive ionic layer deposition, during the oxygen evolution reaction upon water splitting in the alkaline medium. *Nanosystems: Phys. Chem. Math.*, 2018, **9**, P. 669–675.

[32] Popkov V.I., Almjasheva O.V., et al. Crystallization behavior and morphological features of $YFeO_3$ nanocrystallites obtained by glycine-nitrate combustion. *Nanosystems: Phys. Chem. Math.*, 2015, **6**, P. 866–874.

[33] Popkov V.I., Almjasheva O.V. Formation mechanism of $YFeO_3$ nanoparticles under the hydrothermal conditions. *Nanosystems: Phys. Chem. Math.*, 2014, **5**, P. 703–708.

[34] Popkov V.I., Tolstoy V.P. Peroxide route to the synthesis of ultrafine CeO_2–Fe_2O_3 nanocomposite via successive ionic layer deposition. *Heliyon*, 2019, **5**, e01443.

[35] Shinagawa T., Garcia-Esparza A.T., Takanabe K. Insight on Tafel slopes from a microkinetic analysis of aqueous electrocatalysis for energy conversion. *Sci. Rep.*, 2015, **5**, 13801.